

Neoclassical Transport Caused by Collisionless Scattering across an Asymmetric Separatrix

Daniel H. E. Dubin and C. F. Driscoll

Department of Physics, University of California, San Diego, La Jolla, California 92093, USA

Yu. A. Tsidulko

Budker Institute of Nuclear Physics, Novosibirsk, Russia

(Received 16 June 2010; published 27 October 2010)

Plasma loss due to apparatus asymmetries is a ubiquitous phenomenon in magnetic plasma confinement. When the plasma equilibrium has locally trapped particle populations partitioned by a separatrix from one another and from passing particles, the asymmetry transport is enhanced. The trapped and passing particle populations react differently to the asymmetries, leading to the standard $1/\nu$ and $\sqrt{\nu}$ transport regimes of superbanana orbit theory as particles collisionally scatter from one orbit type to another. However, when the separatrix is itself asymmetric, particles can collisionlessly transit from trapped to passing and back, leading to enhanced transport.

DOI: [10.1103/PhysRevLett.105.185003](https://doi.org/10.1103/PhysRevLett.105.185003)

PACS numbers: 52.55.Dy, 52.25.Dg, 52.25.Fi, 52.25.Gj

Magnetically confined plasmas often have one or more locally trapped particle populations, either by accident or design, partitioned by separatrices from one another and from passing particles. This paper examines the effect of these trapped particles on neoclassical transport (transport due to external field asymmetries). In the low collisionality regimes associated with fusion plasmas, strong neoclassical transport is caused by particles that cross these separatrices in the presence of magnetic or electrostatic field asymmetries [1–8].

Collisional scattering (at rate ν) is often regarded as the main mechanism driving the separatrix crossing [1–4], leading to standard superbanana transport regimes scaling as $1/\nu$ or $\sqrt{\nu}$. However, in certain cases *collisionless* particle orbits can cross the separatrices. We will show that this results in enhanced transport that is independent of ν and can greatly exceed standard superbanana transport [5].

The physics of the new mechanism and that of superbanana transport are similar. Trapped and passing particles typically experience different error fields because the fields vary spatially and trapping isolates particles in certain spatial regions. Drift orbits for particles trapped along \mathbf{B} in two separate regions are displaced from one another by a distance Δr , because the field errors acting in each region differ, leading to transport as particles randomly transit from trapped to passing and back.

For example, the $\sqrt{\nu}$ superbanana regime occurs for $\nu < \omega_0$ (where ω_0 is the frequency of the drift orbits), and is due to a collisional boundary layer with energy width $\Delta W_c \equiv \sqrt{TV_0\nu/\omega_0}$ that forms around the separatrix energy V_0 separating trapped and passing particles [1,2,5,9,10]. Particles in this boundary layer diffuse between trapped and passing every orbital period, taking steps of order Δr , and leading to a $\sqrt{\nu}$ scaling for the radial diffusion:

$$D_r \sim \omega_0 \eta_\nu \Delta r^2 \propto (\nu/B)^{1/2}, \quad \nu \lesssim \omega_0, \quad (1)$$

where $\eta_\nu \sim \Delta W_c e^{-V_0/T} / \sqrt{V_0 T} \sim \sqrt{\nu/\omega_0} e^{-V_0/T}$ is the fraction of particles in the boundary layer.

Now, however, consider the effect of an asymmetry on the separatrix itself. Such an asymmetry allows particles to cross the separatrix without needing collisions to do so. If the separatrix energy varies along the drift surface from $V_0 - \Delta V$ to $V_0 + \Delta V$, then particles with parallel energies in this range transit between passing and trapped. Every orbital period they are then randomly trapped on either side of the separatrix, and since error fields differ on each side, this leads to transport that scales as

$$D_r \sim \eta_{\Delta V} \omega_0 \Delta r^2 \propto \nu^0 B^{-1}, \quad (2)$$

where $\eta_{\Delta V} \sim \Delta V e^{-V_0/T} / \sqrt{V_0 T}$ is the fraction of particles in the energy range $V_0 - \Delta V$ to $V_0 + \Delta V$ that can collisionlessly transit from trapped to passing. This collisionless diffusion is independent of collision frequency, and hence dominates the transport when $\Delta V > \Delta W_c$, i.e., when $\nu < \omega_0 \Delta V^2 / V_0 T$.

In what follows we sketch a more detailed analysis of this collisionless transport mechanism and discuss the effect of collisions. We then compare the theory to simulations.

Consider a nominally cylindrical plasma column, trapped axially by an electrostatic potential energy ϕ_0 , and trapped radially by a uniform axial magnetic field \mathbf{B} . Particles with charge q and mass M bounce back and forth along the magnetic field and rotate in the θ direction due to the $E \times B$ drift at frequency $\omega_0(r, z) = -(c/qBr)E_r$, where $E_r = -\partial\phi_0/\partial r$. A “squeeze” potential is applied to a central electrode that creates two trapped particle populations, labeled 1 and 2 (Fig. 1). The maximum height of the squeeze potential V_s varies in azimuthal angle θ , because the central electrode is split into sectors that can be

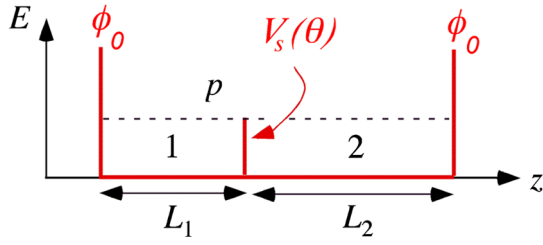


FIG. 1 (color online). Idealized double-well confinement geometry used in the theory and simulations.

biased to different potentials. We assume $V_s(\theta) = V_0 + \Delta V \cos m\theta$. The squeeze is assumed to be very narrow in z so that, by itself, it causes negligible radial transport. This distinguishes this system from some previous work on transport due to separatrix asymmetries [7,8].

Passing particles have axial kinetic energy K larger than V_s and can access both sides of the trap. Trapped particles are trapped on one side of V_s or the other. This double-well potential is analogous to the magnetic wells that occur in stellarators and bumpy tori.

Particles cross the separatrix when K satisfies

$$K = V_s(\theta) = V_0 + \Delta V \cos m\theta. \quad (3)$$

According to Eq. (3) there are m values of θ , θ_{0n} , $n = 0, \dots, m-1$, where the particles become trapped, and m others, θ_{1n} , where they become passing particles:

$$\theta_{(0)n} = \pm \theta_K/m + 2\pi n/m, \quad n = 0, \dots, m-1, \quad (4)$$

where $\theta_K = \cos^{-1}[(K - V_0)/\Delta V]$.

When particles become trapped, we assume that they are trapped in region 1 or 2 with probability p_1 and p_2 , respectively, where $p_1 + p_2 = 1$. For the idealized trap potential shown in Fig. 1, $p_1 = L_1/(L_1 + L_2)$ and $p_2 = L_2/(L_1 + L_2)$.

Radial transport is dominated by a static asymmetry potential $\delta\phi(r, \theta, z)$ that acts over the plasma column to cause radial $E \times B$ drifts. We assume

$$\delta\phi(r, \theta, z) = \varepsilon(r, z) \cos\ell(\theta + \alpha), \quad (5)$$

where α is the phase angle between the asymmetry potential and the separatrix potential. We will see that the collisionless transport depends on α .

The linearized bounce-averaged equations of motion are $d\theta/dt = \bar{\omega}_0$, $dr/dt = (c\ell\bar{\varepsilon}_i/qBr) \sin\ell(\theta + \alpha)$, where the overbar denotes a bounce average: $\bar{\varepsilon}_i$ is the bounce average of ε for $i = 1, 2$ or p (i.e. trapped of type 1 or 2, or passing—see Fig. 1). The value of the bounce average depends on the type of orbit because ε depends on z , and trapped and passing particles average over different z positions. We assume that the plasma “rigidity” $\pi\bar{v}/(\bar{\omega}_0(L_1 + L_2)) \gg 1$, where $\bar{v} \equiv \sqrt{T/M}$ is the thermal speed, so that bounce-averaged dynamics are a good approximation. Otherwise, bounce-rotation resonances neglected here are important [9].

The overall change in r in one rotation period can be found by integration of dr/dt between separatrix crossings:

$$\Delta r = \sum_{n=0}^{m-1} \left[\frac{\bar{\varepsilon}_n}{\bar{E}_r} (\cos\ell(\theta_{1n} + \alpha) - \cos\ell(\theta_{0n} + \alpha)) + \frac{\bar{\varepsilon}_p}{\bar{E}_r} (\cos\ell(\theta_{0_{n+1}} + \alpha) - \cos\ell(\theta_{1n} + \alpha)) \right], \quad (6)$$

where $\bar{\varepsilon}_n$ is a random variable that for each n takes the values $\bar{\varepsilon}_1$ and $\bar{\varepsilon}_2$ with probability p_1 and p_2 , respectively. Then taking the average of Eq. (6) over $\bar{\varepsilon}_n$ and noting $\bar{\varepsilon}_p = p_1\bar{\varepsilon}_1 + p_2\bar{\varepsilon}_2$, we get $\langle \Delta r \rangle = 0$. The radial diffusion coefficient D_r can be obtained from $\langle \Delta r^2 \rangle$ by integrating over the distribution of parallel kinetic energy, $F_0(K)$, which is normalized so that $\int dK F_0 = 1$:

$$D_r = \frac{\bar{\omega}_0}{2\pi} \int_{-\Delta V}^{\Delta V} dK \frac{\langle \Delta r^2 \rangle}{2} F_0(K). \quad (7)$$

By a change of variables from energy K to θ_K , the integral can be performed analytically, assuming that $\Delta V \ll V_0$, so that we may replace $F_0(K)$ by $F_0(V_0)$. The result is

$$D_r = \frac{\bar{\omega}_0 \Delta V}{2\pi} F_0(V_0) \frac{(\bar{\varepsilon}_1 - \bar{\varepsilon}_2)^2}{\bar{E}_r^2} p_1 p_2 \hat{D}_{\ell m}(\alpha), \quad (8)$$

where

$$\hat{D}_{\ell m} = m \frac{4\ell^2 - m^2 \sin^2 \frac{\pi\ell}{m}}{4\ell^2 - m^2} \begin{cases} 1 & \frac{2\ell}{m} \notin \text{integers} \\ 2\sin^2 \ell\alpha & \frac{2\ell}{m} \in \text{integers}. \end{cases} \quad (9)$$

The diffusion coefficient D_r is independent of collision frequency and scales as Eq. (2).

For $\ell = m = 1$, the case considered in Ref. [6], the coefficient \hat{D}_{11} is $(8/3)\sin^2\alpha$, and hence vanishes for $\alpha = 0$ or π , the only cases considered in Ref. [6]. The reason for this can be understood from Eq. (6). For $\alpha = 0$ or π , and $\ell = m = 1$, $\Delta r = 0$ because $\theta_1 = -\theta_0 = \theta_K$ [see Eq. (4)], so there is no net drift step. A sketch of these orbits is shown in Fig. 2(a) (note the similarity to Fig. 2 of Ref. [6]). For $\ell = 1$ the trapped portions of the orbit are shifted circles. Trapped particles move radially, but up-down symmetry implies particles transit from trapped to passing and back at the same radius, so the drift orbit is closed and there is no net radial step. However, when $\alpha \neq 0$, symmetry is broken and particle orbits are trapped and detrapped at different radii, leading to radial steps [Fig. 2(b)]. Of course, for $\alpha = 0$ or π the diffusion does not completely vanish; collisional effects not kept in the above analysis yield finite diffusion consistent with Ref. [6].

Equations (8) and (9) can be regarded as the collisionless limit of a more general theory expression for the transport that includes collisions. The perturbed particle distribution is written as $\delta f = F_0(K)(-\delta\phi + \omega_r g)/T$, where ω_r is the fluid ($E \times B$ + diamagnetic) rotation frequency, and the nonadiabatic part g solves the bounce-averaged Fokker-Planck equation

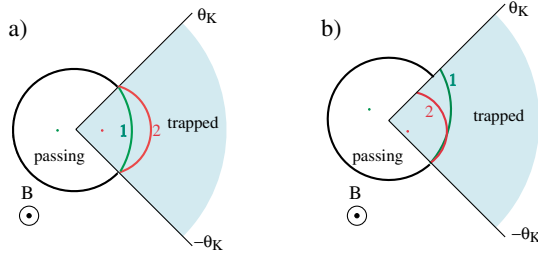


FIG. 2 (color online). Sketch of drift orbits for one drift period beginning at $\theta = \theta_K$, for $\ell = m = 1$. (a) $\alpha = 0$, and (b) $\alpha \neq 0$. Trapped orbit centers (displaced circles) are shown by small dots. At $\theta = -\theta_K$ the passing orbit becomes trapped in either region 1 or 2.

$$\bar{\omega}_0 \partial g / \partial \theta - \hat{C}g = \overline{\partial \delta \phi} / \partial \theta. \quad (10)$$

Here $\hat{C}g = 2V_0 T \nu \partial^2 g / \partial K^2$ is the collision operator, keeping only the highest energy derivative and expanding near $K = V_0$ [1,2,9]. The solution of this driven diffusion equation in the trapped and passing regions yields a radial diffusion coefficient given by Eq. (8), except that $\hat{D}_{\ell m}(\alpha)$ is replaced by $\hat{D}_{\ell m}(\Delta W_c / \Delta V, \alpha)$. For $2\ell/m \in \text{integers}$, $\hat{D}_{\ell m}$ may be written as

$$\Delta V \hat{D}_{\ell m} = \Delta W_c \hat{D}_c + \Delta V \hat{D}_{\Delta V} \sin^2 \ell \alpha, \quad (11)$$

where $\hat{D}_c(\Delta W_c / \Delta V, \ell, m)$ and $\hat{D}_{\Delta V}(\Delta W_c / \Delta V, \ell, m)$ represent the α -independent and α -dependent contributions to the transport.

These functions are plotted in Fig. 3 versus $\Delta W_c / \Delta V$. In the collisionless limit $\Delta W_c \ll \Delta V$, they can be found from Eq. (9): for $\ell = 1$ and $m = 2$, $\hat{D}_c = 0$ and $\hat{D}_{\Delta V} = 4$, while for $\ell = 1$ and $m = 1$, $\hat{D}_c = 0$ and $\hat{D}_{\Delta V} = 8/3$. Furthermore, we find that $\hat{D}_c \rightarrow 0$ as $(\Delta W_c / \Delta V)^p$, with

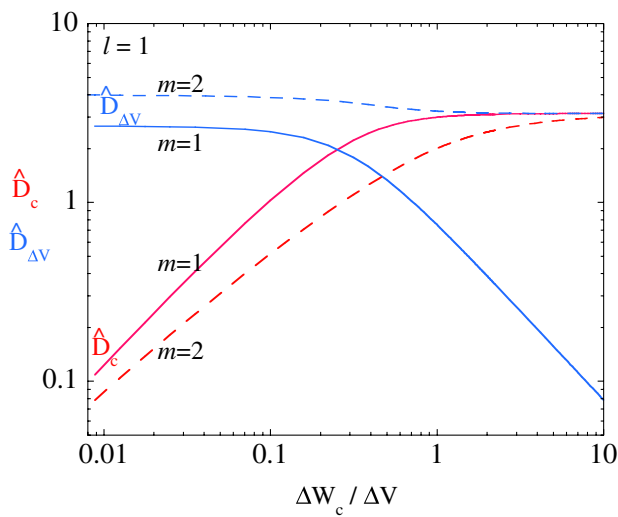


FIG. 3 (color online). Scaled diffusion coefficients versus the ratio of the collisional and collisionless widths, for $m = 1$ (solid line) and $m = 2$ (dashed line), both with $\ell = 1$.

$p \approx 1$ for $\ell = m = 1$, consistent with the results of Ref. [6], and $p \approx 5/6$ for $\ell = 1$ and $m = 2$. In the collisional limit $\Delta W_c \gg \Delta V$, $\hat{D}_c \rightarrow \pi \sqrt{\ell}$, and for $\ell = 1$ and $m = 2$, we get $\hat{D}_{\Delta V} \rightarrow \pi$, while for $\ell = 1$ and $m = 1$, $\hat{D}_{\Delta V} \rightarrow \pi \Delta V / (4 \Delta W_c)$. In this collisional limit, the first term in Eq. (11) dominates, so that transport is proportional to the collisional width ΔW_c , in agreement with Eq. (1).

Simulations of the transport were performed to test the theory, using the method described in Ref. [9]. Equations of motion for $N \sim 5000$ particles were integrated in time in prescribed potentials, including Langevin collisions modeled by a drag force on v_z and a fluctuation in v_z every time step. The confining potential was taken to be the idealized square well shown in Fig. 1, with $L_1 = L_2 \equiv L$, and the asymmetry potential was taken to be $\delta \phi(z, \theta) = \varepsilon \text{sgn}(z) \cos \ell(\theta + \alpha)$, so $-\bar{\varepsilon}_1 = \bar{\varepsilon}_2 = \varepsilon$ and $p_1 = p_2 = 1/2$. Radial diffusion was measured by following the mean square radius, $\sum_i (r_i(t) - r_i(0))^2 = 2ND_r t$.

The diffusion coefficient D_r is plotted in Fig. 4 versus phase angle α for simulation parameters $\ell = m = 1$, $\bar{v} / \omega_0 L = 20$, $\varepsilon / T = 10^{-3}$, $V_0 / T = 0.5$, $\Delta V / T = 0.1$, and $\nu L / \bar{v} = 10^{-5}$. The expected $\sin^2 \alpha$ dependence is observed, and the measured diffusion is well described by the collisionless theory of Eq. (8) (solid line). In Fig. 5 diffusion is plotted versus ν for $\alpha = 1$ and two values of ε ; other parameters are the same. Measured diffusion matches Eq. (11), showing the expected $\sqrt{\nu}$ dependence at large ν . At small ν , D_r is independent of ν , provided ν is not too small and ε is not too large; otherwise, effects not included in the theory become important.

In the limit as $\nu \rightarrow 0$, D_r approaches 0 because the particle distribution relaxes to a BGK equilibrium. In the

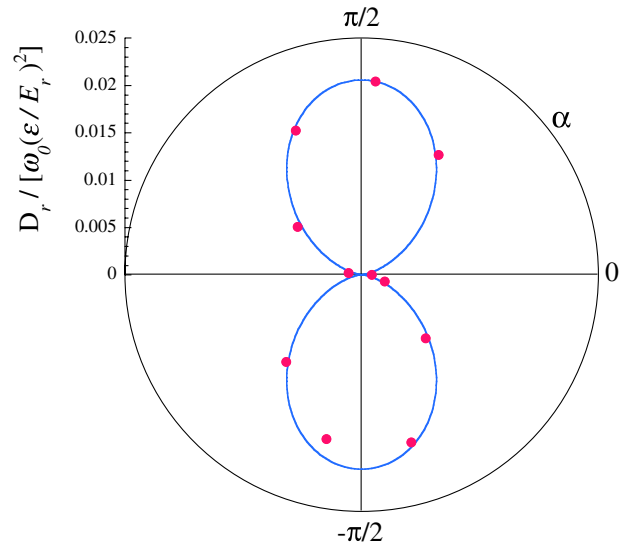


FIG. 4 (color online). Radial diffusion versus phase angle α in simulations (dots) and from collisionless theory, Eqs. (8) and (9), for $\ell = m = 1$.

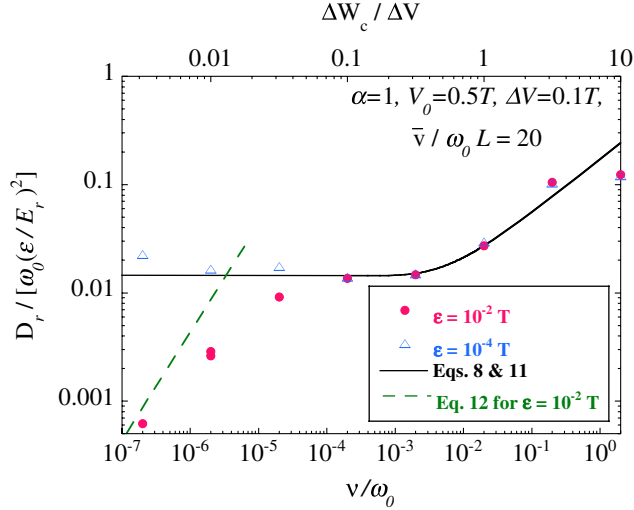


FIG. 5 (color online). Radial diffusion versus collision frequency for two asymmetry amplitudes, $\epsilon = 10^{-2}$ T and $\epsilon = 10^{-4}$ T. Simulations are dots, while the quasilinear theory is a solid line, and the nonlinear “banana” estimate is shown with a dashed line.

collisionless limit, particle motion conserves energy and this limits the total possible change in parallel kinetic energy. Kinetic energies cannot change by more than roughly ΔV since particles would otherwise enter integrable regions of phase space that are either always trapped or always passing. This requires crossing KAM surfaces, which is not allowed in a four-dimensional (guiding center) phase space [11]. Thus, without collisions, phase mixing of the particle distribution eventually yields a stationary (BGK) state. Although Eq. (9) is independent of ν , collisions are implicitly required in order to refresh the distribution and keep it close to Maxwellian form.

To estimate D_r in the low collisionality regime, we first estimate the time τ_r required for collisionless relaxation, as the time needed for a particle to collisionlessly diffuse in kinetic energy by order ΔV due to trapping and untrapping that occurs every rotation period: $\tau_r \sim \Delta V^2 / \bar{\omega}_0 \epsilon^2$. This time is analogous to the wave-trapping time in standard banana-orbit theory; here, however, the orbits are chaotic. Adding collisions drives the particle distribution, flattened over an energy range ΔV around V_0 , back toward a Maxwellian form. The collisional relaxation time τ_c required for this process is $\tau_c \sim \Delta V^2 / \nu V_0 T$.

When $\tau_c < \tau_r$, i.e., when $\nu > \bar{\omega}_0 \epsilon^2 / (V_0 T)$, collisions prevent collisionless relaxation to a BGK state, and this is the regime where the previous theory is valid. When $\tau_c > \tau_r$, one can estimate D_r in the manner of banana-orbit theory. Particles now take large radial chaotic

“banana-orbit” steps $\Delta r \sim \Delta V / \bar{E}_r$ associated with kinetic energy change ΔV , due to multiple separatrix crossings. After a time τ_c these particles are collisionally replaced, leading to radial diffusion $D_r \sim (\Delta r^2 / \tau_c) F_0(V_0) \Delta V$, where $F_0 \Delta V$ is the fraction of particles participating. Substituting for Δr and τ_c yields

$$D_r \sim 10\nu \left(\frac{\Delta V}{\bar{E}_r} \right)^2 \frac{\sqrt{V_0 T}}{\Delta V} e^{-V_0/T}, \quad \nu < \frac{\bar{\omega}_0 \epsilon^2}{V_0 T}, \quad (12)$$

where the prefactor of 10 is chosen to provide a reasonable fit to the simulation data (Fig. 5).

We have seen that enhanced transport due to collisionless scattering across a separatrix supercedes standard $\sqrt{\nu}$ superbanana transport, and is independent of ν when $\epsilon^2 \lesssim \nu V_0 T / \bar{\omega}_0 \lesssim \Delta V^2$ (assuming $\bar{v} / \bar{\omega}_0 L \gg 1$). For ν smaller than this range, a novel “chaotic banana” regime sets in with transport roughly proportional to ν . This transport mechanism could be an important loss process in many systems with asymmetric separatrices such as stellarators. The mechanism also causes various other effects, such as growth or damping of plasma modes. These effects will be considered in several following papers [12]. The transport depends on the relative phase of the field errors, which can be a strong experimental signature of the effect if this phase is controllable.

This work was supported by National Science Foundation Grant No. PHY-0903877 and Department of Energy Grant No. DE-SC0002451.

-
- [1] M. N. Rosenbluth, D. W. Ross, and D. P. Kostamurov, *Nucl. Fusion* **12**, 3 (1972).
 - [2] T. J. Hillsbeck and T. M. O’Neil, *Phys. Plasmas* **10**, 3492 (2003).
 - [3] A. H. Boozer, *Phys. Fluids* **23**, 2283 (1980).
 - [4] J. W. Connor and R. J. Hastie, *Phys. Fluids* **17**, 114 (1974).
 - [5] H. Mynick, *Phys. Plasmas* **13**, 058102 (2006).
 - [6] H. Mynick, *Phys. Fluids* **26**, 2609 (1983).
 - [7] J. R. Cary and D. L. Bruhwiler, *Proceedings of the 12th IEEE Particle Accelerator Conference*, edited by E. Lindstrom and L. Taylor (IEEE, New York, 1987), p. 1290.
 - [8] V. S. Marchenko, *Nucl. Fusion* **35**, 69 (1995).
 - [9] D. H. E. Dubin, *Phys. Plasmas* **15**, 072112 (2008).
 - [10] D. H. E. Dubin, *AIP Conf. Proc.* **1114**, 121 (2009).
 - [11] A. J. Lichtenberg and M. A. Lieberman, *Regular and Chaotic Dynamics* (Springer-Verlag, New York, 1991), p. 61.
 - [12] A. A. Kabantsev, C. F. Driscoll, D. H. E. Dubin, and Yu. A. Tsidulko, *Phys. Rev. Lett.* (to be published).